HHS Public Access

Author manuscript

J Physiol. Author manuscript; available in PMC 2021 December 01.

Published in final edited form as:

J Physiol. 2020 December ; 598(23): 5541–5554. doi:10.1113/JP280276.

Acute Activation of Bronchopulmonary Vagal Nociceptors by Type I Interferons

Mayur J. Patil[1], **Fei Ru**[1], **Hui Sun**[1], **Jingya Wang J**[3], **Roland R. Kolbeck R**[3], **Xinzhong Dong**[2], **Marian Kollarik**[1], **Brendan J. Canning**[1], **Bradley J. Undem**[1]

[1]The Johns Hopkins School of Medicine Departments of Medicine, Baltimore MD

[2]The Johns Hopkins School of Medicine Departments of Neuroscience, Baltimore MD

[3]AstraZeneca BioPharmaceuticals R&D Gaithersburg, MD

Abstract

We evaluated the ability of type I interferons to acutely activate airway vagal afferent nerve terminals in mouse lungs. Using single cell RT-PCR of lung-specific vagal neurons we found that IFNAR1 and IFNAR2 were expressed in 70% of the TRPV1-positive neurons (a marker for vagal C-fiber neurons) and 44% of TRPV1-negative neurons. We employed an *ex vivo* vagal innervated mouse trachea-lung preparation to evaluate the effect of interferons in directly activating airway nerves. Utilizing 2-photon microscopy of the nodose ganglion neurons from *Pirt-Cre;R26-GCaMP6s* mice we found that applying IFNα or IFNβ to the lungs acutely activated the majority of vagal afferent nerve terminals. When the type 1 interferon receptor, IFNAR1, was blocked with a blocking antibody the response to IFNβ was largely inhibited. The type 2 interferon, IFNγ, also activated airway nerves and this was not inhibited by the IFNAR1 blocking antibody. The Janus kinase inhibitor GLPG0634 (1 μM) virtually abolished the nerve activation caused by IFNβ. Consistent with the activation of vagal afferent C-fibers, infusing IFNβ into the mouse trachea led to defensive breathing reflexes including apneas and gasping. These reflexes were prevented by pretreatment with an IFN type-1 receptor blocking antibody. Finally, using whole cell patch-clamp electrophysiology of lung-specific neurons we found that IFNβ (1000 U/ml) directly depolarized the membrane potential of isolated nodose neurons, in some cases beyond to action potential threshold. This acute non-genomic activation of vagal sensory nerve terminals by interferons may contribute to the incessant coughing that is a hallmark of respiratory viral infections.

Corresponding Author Bradley Undem, Johns Hopkins Asthma and Allergy Center, 5501 Hopkins Bayview Circle, Baltimore, Maryland 21224, bundem@jhmi.edu, 410-550-2160.

Author's Contributions

MJP and BJU contributed to the conception or design of the study, acquisition, analysis or interpretation of data for the work, and drafting the manuscript or revising it critically for important intellectual content. MJP, FR, HS, MK and BJU contributed to the acquisition, analysis or interpretation of data for the study, and drafting the manuscript or revising it critically for important intellectual content. All authors approved the final version of the manuscript, agree to be accountable for all aspects of the work in ensuring that questions related to the accuracy or integrity of any part of the work are appropriately investigated and resolved, all persons designated as authors qualify for authorship, and all those who qualify for authorship are listed.

Competing interests

The authors declare that they have no competing interests.

Keywords

IFNβ; IFNα; Vagal afferents; interferons; IFN type I receptors; 2-photon; IFNγ; airway lung nerve terminals; vagal C-fibers; cough

Introduction

Coughing is a common feature of respiratory viral infections. By evoking cough, the virus can evade the immune system and spread to other hosts. The urge to cough sensations associated with respiratory viral infections are most likely due to the activation of a subset of sensory nerves terminating in the airway mucosa referred to as vagal sensory C-fibers (Canning *et al.*, 2014). There is little evidence that respiratory viruses directly activate vagal sensory C-fibers. It is more likely that viral infection leads to the production of inflammatory mediators and cytokines in the airways that in turn activate the nerves.

Vagal C-fibers that innervate the airway are often TRPV1 expressing, capsaicin-sensitive nerves. In an attempt to determine which mediators or cytokines are most likely to be involved in directly activating these nerves we recently carried out a transcriptome analysis of capsaicin-sensitive and TRVP1 expressing vagal visceral C-fiber neurons and quantified the gene expression for cytokine and mediator receptors. We noted that the receptors for chemokines or cytokines were rarely expressed with the notable exception of strong expression of type 1 and type 2 interferon receptor (IFNRs) (Wang *et al.*, 2017). In addition, we noted that the type 1 interferon IFNβ and type 2 interferon IFNγ caused an immediate elevation in intracellular calcium at the level of the sensory neuron cell body. If IFNs, known to be strongly induced in the airways during most respiratory virus infections, reach the cell bodies in the distant vagal ganglia they could phenotypically alter C-fiber neurons by activating or suppressing IFN-sensitive genes. Others have indeed provided evidence for a role for IFNs in growth and differentiation of sensory neurons situated in the dorsal rot ganglia (DRG) (Neumann *et al.*, 1997; Golz *et al.*, 2006).

Histological evidence supports the hypothesis that IFN receptors (IFNRs) synthesized in sensory cell bodies can be transported both centrally and peripherally (Vikman *et al.*, 1998). A major unaddressed question, however, is whether activation of IFN receptors at the level of C-fiber nerve terminals in peripheral tissues (the business end of sensory nerves) can overtly activate the nerves to cause sensations and reflexes? More specifically, can IFNs in the airways lead to action potential discharge in vagal C-fibers with intensities sufficient to cause respiratory reflexes? This is the key question that we address here. The data obtained support the hypothesis that type 1 interferons IFNα and IFNβ, via stimulation of the type 1 IFN receptors in the nerve terminals and activation of JAK1, acutely evoke action potential discharge in vagal broncho-pulmonary C-fiber terminals. Interferons may therefore play a role in viral infection-induced coughing and other reflexes, independently of their effects on gene regulation.

METHODS

Ethical approval

All animal experiments were approved by the Institutional Animal Care and Use Committee (IACUC) at the Johns Hopkins School of Medicine (IACUC Animal protocol number: MO19M151). We as investigators understand the ethical principles under which the journal operates, and our work complies with the animal ethics checklist as described in the editorial by Grundy (Grundy, 2015).

Animals

Male mice (C57BL/6J) were purchased from Jackson Labs. The Pirt-Cre mice were generated in X. Dong's laboratory (Han *et al.*, 2018). The ROSA26-lsl-GCaMP6s line was originally provided by D. Bergles at The Johns Hopkins University and is now available in Jackson Labs. The animals were housed in an approved animal facility under a 12:12h light/dark cycle with controlled temperature and humidity, in groups in cages providing unrestricted access to food and water and an appropriate environmental enrichment. On the day of the experiments the mouse was I.P. injected with anti-coagulant heparin (2000 IU kg −1; diluted in saline 1000 IU ml−1). The injection of heparin is given to prevent blood clot formation and improves blood removal from the pulmonary circulation. After 15–20 min, the mice were euthanized by exposure to CO_2 in a rising concentration and exsanguination. The CO_2 was administered at a flow rate, measured by flow meter, displacing #20–30% of the chamber volume per minute conforming to Grundy, 2015. The vagal-lung preparations were studied at 37°C in Krebs bicarbonate solution (KBS); composed of (mM): 118 NaCl, 5.4 KCl, 1.0 NaH_2 PO_4, 1.2 $MgSO_4$, 1.9 $CaCl_2$, 25.0 $NaHCO_3$ and 11.1 dextrose, gassed with air mix (95%O_2–5%CO_2, pH 7.4).

Retrograde labelling and cell dissociation

To collect lung-specific bronchopulmonary afferent neurons from jugular/nodose ganglia, the airways of C57/BL6 mice (male, 8 weeks) were retrogradely labelled using WGA 488 (W11261, Invitrogen) (1% DMSO in sterile DPBS, Invitrogen). The mice were anesthetized using 2 mg ketamine and 0.2 mg xylazine I.P. per mouse. The effect of the anesthetic was confirmed by checking for tail reflex after pinching. The anesthetized mice were then orotracheally intubated, and 20ul of WGA 488 was instilled into the tracheal lumen 4–5 days before an experiment. The mice were injected with a reversal agent to aid in recovery from the anesthetic. The mice were provided with liquid food after the procedure and monitored for any signs of distress after the dye instillation for 2 days. The animals were euthanized by CO_2 asphyxiation, and the jugular/nodose ganglia were dissected and cleared of adhering connective tissue. Isolated ganglia were incubated in an enzyme buffer (2 mg ml −1 collagenase type 1A and 2 mg ml−1 dispase II in Ca^{2+}-, Mg^{2+}-free Hanks' balanced salt solution) for 30–60 min at 37°C. Neurons were dissociated by trituration with three glass Pasteur pipettes of decreasing tip pore size, then washed by centrifugation (three times at 1000 g for 2 min) and suspended in L-15 medium containing 10% fetal bovine serum (FBS, Invitrogen). The cell suspension was transferred onto poly-D-lysine/laminin-coated coverslips. After the suspended neurons had adhered to the coverslips for 2 h, the neuron-attached coverslips were flooded with the L-15 medium (10% FBS) and used within 8 h for

cell picking. In our previous studies (Kollarik *et al.*, 2003) we compared the results from single cell RT-PCR (scRT-PCR) of the neurons retrogradely labeled from the lung with the results from electrophysiological studies of afferent fibers innervating the lung. We observed that the lung afferent subtype populations were similarly represented by scRT-PCR and electrophysiology, suggesting that there are no substantial differences in accessibility of nerve terminal phenotypes to the injected dye.

Cell picking

Coverslips of retrogradely labelled, dissociated neurons were constantly perfused by Locke's solution and the labelled cells identified by using fluorescence microscopy. Single cells were sucked into a glass-pipette (tip diameter 50–150 μm) that was pulled with a micropipette puller (Model P-87, Sutter Instruments Co., Novato, CA, USA) by applying negative pressure. The pipette tip was then broken in a PCR tube containing 1 μl RNAse Inhibitor (RNAseOUT, Invitrogen, 2 U μl −1), immediately snap frozen and stored on dry ice. From one coverslip, one to four cells were collected. A sample of the bath solution from the vicinity of a labelled neuron was collected from each coverslip for no-template experiments (bath control).

Single-cell RT-PCR

The tubes with airway/lung-labelled jugular/nodose single cells suspended in RNAse OUT was used to synthesize first strand cDNA by using the SuperScript III First-Strand Synthesis System for RT-PCR (Cat#18080044, Invitrogen, Carlsbad, CA, USA) according to the manufacturer's recommendations. In short, cell samples were defrosted and then oligo(dT) and random hexamer primers (Roche Applied Bioscience) were added and tubes incubated for 10 mins at 75°C. 22 μl of the volume was reverse transcribed by adding SuperscriptIII RT for cDNA synthesis, whereas water was added to the remaining sample, which was used as –RT control. 1 μl (cDNA, RNA control or bath control) was used for PCR amplification of mouse β-actin, TRPV1, P2X2, IFNAR1 and IFNAR2 by the HotStar Taq Polymerase Kit (Qiagen) according to the manufacturer's recommendations in a final volume of 20 μl. After an initial activation step at 95°C for 15 min, cDNAs were amplified with custom-synthesized primers (Sigma-Aldrich) (Table 1) by 50 cycles of amplification. The PCR program used was, denaturation at 94°C for 30 s, annealing at 60°C for 30s and extension at 72°C for 1 min followed by a final extension at 72°C for 10 min. PCR products were then visualized in ethidium bromide-stained 1.5% agarose gels. For details on the RNA SEQ analysis please see our previous study (Wang *et al.*, 2017).

Two-Photon imaging

The trachea, lungs and vagus nerves, including the ganglia, were isolated and prepared for the study of nerve activation as we have previously described (Kollarik *et al.*, 2003; Patil *et al.*, 2019). The trachea and lungs were isolated from *Pirt-Cre;R26-GCaMP6s* transgenic mice. The isolated lungs were washed with KBS to wash the blood from the pulmonary circulation. A 2-compartment chamber/tissue bath was used to mount the trachea and right and left lungs with intact right or left side extrinsic vagal innervation including right or left jugular and nodose ganglia. The right or left nodose and jugular ganglia along with the vagus nerve were placed in one compartment, with the lung and trachea in the second

compartment. The two compartments were separately superfused with KBS (3–4 mL min–1 at 37°C). There was no fluid exchange between the two compartments. The lung was pinned in one compartment (airway chamber) to receive chemical stimuli. The trachea was cannulated with PE tubing and continuously perfused with KBS (4 and mL min–1, respectively). The drugs or vehicle were added to the receptive field in the lung via the trachea. The drugs applied in the lungs leave slowly in the perfusing buffer solution via small puncture ports made in the lungs and get immediately diluted into the superfusion buffer. The left or right vagal ganglia were pinned in a second compartment (VG chamber) for 2-photon imaging. The chamber containing the tissue preparation is mounted on the microscope stage and fixed in place with 2 screws. The 2 chambers are then connected to buffer inlet lines perfusing warm buffer (37 °C), heated via Warner instruments heating elements. The flow of KBS, gassed with air mix (95%O_2–5%CO_2, pH 7.4), was maintained at 3–4ml per min. The 20X objective (Scientifica) was positioned directly above the nodose ganglia in the small chamber. Using Labview software the ganglia coordinates for Z stack, starting from top to bottom (100 microns) were adjusted. The piezo drive for the objective was engaged and the objective positioned at the top of the ganglia ready for image acquisition. We acquire live images of the nodose ganglia at 10 frames with 600 Hz frame scan mode per 6 s at a depth of ~100μm (10 planes of 10 μm thick slices Fig 1, A). During the recordings we noticed that we could observe the activity of ~1000 neurons in the ganglia. Our experiments revealed that ~10% of the total neurons are lung-specific. In order to calibrate the 2-photon system for our *ex vivo* preparation we carried out extensive electrical stimulation of the vagus nerve and analyzed the Ca^{2+} transients to show that the intensity of the response is quasi-linear between 1Hz and 10 Hz stimulation. First, we record baseline activity of the neurons without any stimulation and adjust the laser power and emission gain (of the PMT) to record lowest signal to noise ratio. The laser power and gain for our system was adjusted at 35% and 750 volts respectively. Next, we deliver 1ml of buffer into the lungs and record activity of neurons that are positive for distention. We mark these neurons during data analysis and did not include them in our drug response analysis. The 2-photon setup uses a laser excitation wavelength of 920nm thus there is no photobleaching of the GCaMP6 and hence no loss of signal over repetitive stimulation (Chen *et al.*, 2013). The drugs (1ml volume) were applied into the lungs via the tracheal cannula for 20–30s. The drug response was recorded for a total of 3–5 mins. The lungs were washed with 2ml of KBS in-between every drug application. The baseline for analysis was recorded 30s before every drug application. The number of responding neurons are counted as those that have fluoresce intensity of >1.5-fold over baseline. The software recorded images in tiff files that were analyzed offline using ImageJ (Fiji). Data is presented as $\Delta F/F_0$ (Y axis) over time, the change in fluorescence intensity from baseline. In preliminary experiments, as expected, we noted that severing the vagus nerve prevented the intra-tracheal stimulants from activating ganglion neurons.

Two-Photon imaging data analysis

The nodose ganglia is imaged up to a depth of 100 microns. The 100-micron depth is imaged in increments of 10 microns (1 plane). So altogether 10 planes are imaged in 6 secs (per cycle). Typically, 1–2 cycles of images are collected as baseline (F_0) before any drug is applied. Images are collected for ~3–5 mins during drug application. All images are

exported as tiff files to ImageJ (Fiji) for offline analysis. The first step in ImageJ is to open the Z-stacks of the various applications individually and observe the time lapse images using group Z-stack compression. This observation reveals if there was any X, Y or Z axis movement of the ganglia during recording. Any movement of the ganglia during recording is corrected using an ImageJ plugin Stackreg. Next the Z-stacks for multiple drug analysis are concatenated (stitched) together in the sequence they were applied. The concatenated images are then divided or separated into substacks (each Z stack is divided by 10 to create a substack) which are separated by 20 microns. The 20-micron separation is chosen as it gives enough separation between stacked neurons in the ganglia (mouse sensory neurons are approximately 20-micron in diameter). Thus 5 substacks out of the 10 are analyzed, which ensures the same neurons are not counted twice. The substacked images are used to mark the ROIs (responsive neurons) and the intensity values collected and then analyzed further in excel to calculate the $\Delta F/F_0$ value (change in fluorescent intensity from baseline).

Head-out whole-body plethysmography (Mouse breathing behavior)

Mouse breathing behavior changes in response to the application of drugs to the airways was carried out using head-out whole-body plethysmography as previously described (Chou *et al.*, 2008; Han *et al.*, 2018). In short mice were anesthetized with urethane (1.5 g/kg urethane i.p), which produces a deep anesthesia lasting far longer than the maximum of 2 h of experimentation and were spontaneously allowed to breathe. Adequate anesthesia was confirmed throughout the experiment by monitoring responses to pinching of a hindlimb. Anesthetized mice were secured supine on a warming pad and their extrathoracic trachea was cannulated with a bent luer stub adaptor (cannula). Care was taken to preserve the innervation and vasculature of the trachea. The body of the animal was kept in a sealed chamber and the respiratory effort was monitored digitally using a Biopac data acquisition system. A pressure transducer attached to a side port in the tracheal cannula monitored respiratory efforts. When the surgery was complete, animals were allowed to breathe spontaneously and without any further manipulations for 5 min. Drugs were applied directly into the trachea through the cannula (2ul total volume). The delivery of the drugs directly into the trachea avoids interference from the nasal respiratory tract, which is mainly innervated by trigeminal sensory neurons. Respiratory pauses and augmented breaths were counted from the respiratory waveform offline with AcqKnowledge software. The mice were euthanized using CO_2 asphyxiation after the experiment was complete.

Patch clamp recording

Amphotericin B-perforated whole-cell patch clamp technique on current-clamp mode was employed to record the membrane potential using an Axopatch 200B amplifier interfaced with Axon Digidata 1550A and driven by pCLAMP 10 software (Molecular Devices, Sunnyvale, CA, USA). The experiments were performed at room temperature. Bath solution contained (mM): NaCl 135, KCl 5.4, MgCl2 1, CaCl2 1, HEPES 10 and glucose 10 with pH adjusted to 7.35 with NaOH. Pipette solution contained (mM): KCl 40, K-gluconate 105 and HEPES 10 with pH adjusted to 7.2 with KOH. Freshly prepared amphotericin B was added to the pipette solution (300 μg ml−1) before experiments. The junction potential (12.9 mV estimated using Clampex calculator) was corrected offline.

Statistical analysis

The 2-photon data is presented as the mean intensity of activated neurons in presence of indicated stimuli and expressed as the mean ± SD. In 2-photon experiments drug groups were paired observations whereas the antagonists and antibody treatments were unpaired observations. We used paired and unpaired t-tests and ANOVA to ascertain statistical significance between groups. The specific statistical tests used are indicated in the figure legends as appropriate. Graphpad Prism 7 (GraphPad Software, La Jolla, CA) was used for all the statistical analyses.

Chemicals, Drugs and solutions: All compounds and drugs used were freshly prepared, from stock solutions stored at −20°C, in KREB's solution to their final working concentration on the day of the experiment. α,β-methylene ATP, and capsaicin were purchased from Tocris. Filgotinib (GLPG0634), JAK1 inhibitor was purchased from Selleckchem. Mouse interferons (β, and γ) were purchased from PBL assay science. Interferon type I receptor blocking antibody murine anti-(IFNAR Ab 5A3) and murine control IgG1 antibody (1A7) was obtained AstraZeneca.

RESULTS

Type I interferon receptors are found to be abundantly expressed by airway-specific vagal neurons

We have previously noted in our RNAseq analysis specifically of capsaicin-sensitive nodose and jugular vagal sensory neurons, that most cytokine and chemokine receptors were not expressed, whereas the mRNA for type1 and type 2 interferon receptors was richly expressed (Wang *et al.*, 2017). Here, we evaluated the extent to which *airway specific* vagal sensory neurons express type I IFN receptors, IFNAR1 and IFNAR2, using single cell rt-PCR of neurons retrogradely labeled from the lungs (Fig 1, a, and see Fig S1). Among the 38 neurons investigated, 52% expressed TRPV1 mRNA (a marker for C-fiber neurons). IFNAR1 and IFNAR2 were expressed in 70% of the TRPV1 positive neurons and 44% of TRPV1 negative neurons. The vagal sensory ganglion complex comprises both placodal derived nodose neurons and neural crest derived jugular neurons (schematic in Fig 1, a) (Mazzone & Undem, 2016). We previously have shown that with respect to airway innervation the purinergic P2X2 receptor mRNA is a marker for nodose neurons; failure to express P2X2 is indicative of the neural crest-derived (wnt-1 expressing) airway jugular C-fiber neurons (Nassenstein C, 2010; Wang *et al.*, 2017). Consistent with previous observations (Nassenstein C, 2010), the vast majority (79%) of airway specific neurons isolated from the vagal ganglion complex were nodose neurons. There were only 3 TRPV1 positive P2X2 negative neurons among the 38 cells evaluated. Each of these presumed jugular C-fiber neurons expressed IFNAR1, but only 1 also expressed IFNAR2.

2-photon microscopy using GCaMP6s is useful for evaluating acute activation of airway afferents

The action potentials arising from the airway afferent terminals in the lung invade the cell soma in transit to the central terminals in the brain stem. The action potential leads to calcium entry into the cell body via voltage-gated calcium channels. Phosphoinositide-

interacting regulator of TRP (pirt) is expressed nearly uniformly in mouse vagal sensory neurons (Kim *et al.*, 2020; Mazzone *et al.*, 2020). Therefore, in order to have the calcium indicator expressed in the relevant neurons the tissue was dissected from a *Pirt-Cre;R26-GCaMP6s* mice (Patil *et al.*, 2019). Our vagal-innervated *ex vivo* mouse lung-nerve preparation (Kollarik *et al.*, 2003; Patil *et al.*, 2019) was set up with a 2 photon-microscope objective positioned over the central portion of vagal sensory ganglion complex (Fig 3, a). The central region of the ganglion complex comprises mostly nodose neurons, but generally also includes a small number of jugular neurons (Nassenstein *et al.*, 2010). In our preliminary experiments we stimulated the distal end of the vagus nerve to determine the extent of GCaMP6s expression and the sensitivity of the assay. We noted that virtually all neurons in the ganglion responded when their peripheral axons were stimulated, revealing a near universal expression of the GcaMP6s in the sensory neurons. A sufficient amount of calcium enters the soma with a single action potential to interact with the GCaMP6s in a manner that can be detected by the microscope. The intensity of the fluorescence was proportional to the frequency of action potential discharge between 0.5–10 Hz when stimulated for 20 s (see Fig 2, B). The decay of the fluorescence after the 10 Hz stimulation ended had a first-order rate constant of 60±2.8 ms-1 (n=161 neurons).

Type I interferons are capable of acutely activating airway afferents

IFNα and IFNβ are activators of the type 1 IFN receptor (INF-α receptors comprising IFNAR1 and IFNAR2 chains). IFNβ acutely activated vagal afferent nerve terminals in the lungs. Data summarized in Figure 3 illustrate the effect of IFNβ on vagal nerve terminals in the airways. When 1 ml (100 U/ml) of IFNβ was infused into the lung via the trachea, the action potential discharge was not different than vehicle. However, when 1000 U/ml was infused action potential discharge was noted in a majority of chemically (capsaicin and or α,β, m-ATP)-sensitive airway sensory nerves (static image in Fig 3, b, and 3, e. For video see Video 1). The magnitude of the response (based on intensity of fluorescence in the responding neurons) was similar to that seen by subsequent stimulation, in the same preparation, with the nodose C-fiber activators α,β, m-ATP and capsaicin (Fig 3, e). Increasing the IFNβ concentration to 10,000 U/ml did not increase the magnitude of the response (Fig 3, f). Consistent with the single cell rt-PCR data, IFNβ stimulated ~70% of capsaicin responsive airway-specific neurons (Fig 3, d). Also consistent with the rt-PCR data, IFNβ stimulated 32% of airway nodose (α,β, m-ATP responding) fibers that were capsaicin-*insensitive* (data not shown). As mentioned in our methods section, airway-specific nodose neurons make up about 10% of the total number of neurons in the ganglia. Thus, the percentages, of IFN or CAP sensitive neurons, mentioned throughout are not of the whole ganglia but only airway-specific neurons. IFNα, another type 1 interferon, mimicked IFNβ in activating the vagal afferent nerves in the lungs (Fig 4).

Type I interferon receptors and JAK1 kinase are required and essential for the acute activation of airway-afferents mediated by type I interferons

Although 1000U/ml activated the nerves, the concentration of IFNβ at the receptive fields in the airways cannot be determined when a brief bolus exposure of the interferon is presented via the trachea in our perfusion system. To determine whether the effect was indeed dependent on IFN receptor activation we evaluated a Type 1 receptor blocking antibody.

When IFNAR1 was blocked with a blocking antibody (Peng *et al.*, 2015), the response to IFNβ was largely inhibited, whereas an isotype control antibody had no significant blocking effect (Fig 5, a). The blocking antibody did not inhibit the response to capsaicin (68% capsaicin sensitive neurons with mean intensity of 5.4 in the absence of blocking antibody and 66% capsaicin sensitive neurons with mean intensity of 5.3 in the presence of the antibody), so the data are expressed as % of capsaicin-sensitive nerves responding to IFNβ (Fig 5, b). In our previous RNAseq paper we also noted that the type 2 IFN receptors IFNGR1 and IFNGR2 are expressed in a subset of vagal nociceptors (Wang *et al.*, 2017). It was therefore not surprising that IFNγ mimicked IFNβ in evoking action potential discharge in vagal nociceptive terminals in the lungs (Fig 5, b). Reflecting its specificity, the IFNAR1 blocking antibody did not inhibit the response to IFNγ (Fig 5, a, b).

Intracellular signaling via type I IFN receptors generally requires activation of Janus kinases JAKs (Secombes & Zou, 2017). We data mined our previous RNA SEQ analysis (Wang *et al.*, 2017) for the expression of JAKs and found that the capsaicin sensitive nodose nociceptors express JAK1, but not JAK2 or JAK3 (Fig 5, c). We used GLPG0634 (1 μM) (Van Rompaey *et al.*, 2013) to inhibit JAK1 activity and found that it virtually abolished the response to IFNβ (Fig 5, d, e). As one would expect, GLP0634 did not significantly alter the response to capsaicin which stimulated 61.2 ± 10.8% and 58 ± 11.3% (mean ± *SD*) of lung specific nerves in control and GLP pretreated lungs, respectively (P >0.1) (not shown).

IFNβ is capable of evoking defensive reflexes when administered in the airways of mice

To determine if the C-fiber activation by IFNβ was sufficient to evoke classical vagal C-fiber defensive reflexes we monitored the rate and depth of breathing of anesthetized mice. In this assay intratracheal application of C-fiber stimulants like capsaicin evoke respiratory reflexes comprised of brief episodes of respiratory pauses (apneas) and augmented breaths (gasps) (Chou *et al.*, 2008; Han *et al.*, 2018). Infusing 2 μl of vehicle into the mouse trachea, via a tracheal cannula, lead to an immediate cessation of breathing for ~ 1 sec, followed by a resumption of normal respiration (Fig 6, a). This is likely a reaction to the physical aspect of instilling a liquid into the trachea. Infusing 2 μl of IFNβ into the trachea led to the same immediate cessation of breathing, but this was followed by apneas and gasps, consistent with vagal C-fiber mediated defensive reflex behavior (Fig 6, a, b). These reflexes were prevented by pretreatment with the IFN type-1 receptor blocking antibody (summarized in Fig 6).

The activation of vagal neurons mediated by IFNβ is a result of direct acute action

The quick onset of the response of the nerve terminals to IFNβ when applied to the lungs is indicative of a direct effect on the nerves, and not secondary to effects on other cell types in the lungs. To add credence to this supposition we dissociated nodose neurons from the vagal ganglion and evaluated the effect of IFNβ on individual patch-clamped neurons studied in the absence of other cell types. Bath perfusion of IFNβ (1000 U/ml) for 2–3 mins caused membrane depolarization in 7 out of 7 mouse nodose neurons studied (5 capsaicin-sensitive and 2 capsaicin-insensitive, 3 of the 5 capsaicin-sensitive neurons are labeled from the lungs), averaging from −63.9±5 to −52.9±3.2 mV (p=0.009, paired t-test). The depolarization reached the steady-state slowly, varying from 51 to 192 sec (averaged 131

sec). In 4 out of 7 neurons (3 cap-sensitive and 1 cap-insensitive), IFNβ evoked action potential firing with the mean peak frequency at 3.9±3.2Hz. One example is shown in Fig 7.

DISCUSSION

The data provide evidence for activation of bronchopulmonary nociceptive nerve terminals as a potential contributing factor in interferon-mediated vagal defensive reflex mechanisms. The results reveal that IFNγ, IFNα and IFNβ directly cause acute action potential discharge in C-fibers terminating in mouse lungs. We probed more deeply the effect of IFNβ for mechanistic insights. With respect to IFNβ, the data reveal that this is secondary to type 1 IFN receptor stimulation. The canonical signaling pathways for IFNRs includes the activation of Janus kinase-signal transducer and activator of transcription proteins (JAK-STAT) signaling (Schneider *et al.*, 2014). The data from the sensory nerve terminals supports a role of JAK1 activation, but instead of interacting with transcription proteins, JAK1 ultimately leads to activation (or inhibition) of ion channels that depolarize the terminal membrane to action potential threshold.

The single-neurons rt-PCR results showing IFNR1 and IFNR2 mRNA expression specifically in airway-labeled vagal sensory neurons are consistent with our previous RNAseq analysis of unlabeled nodose and jugular C-fiber neurons (Wang *et al.*, 2017). The data are also largely in keeping with the findings of a recent study of single-cell RNAseq analysis of 88 airway specific vagal sensory neurons (Mazzone *et al.*, 2020). Previous studies have shown that both type 1 and type 2 IFN receptors are also expressed in sensory neurons in the dorsal root ganglion. Moreover, these receptors appear to be transported towards the central and peripheral terminals (Neumann *et al.*, 1997; Vikman *et al.*, 1998; Liu *et al.*, 2016). Information regarding the consequence of stimulating these receptors in sensory neurons is sparse. At the sensory cell body, activation of type 2 interferon receptors can activate JAK- STAT1 signaling which may lead to changes in cell growth and differentiation (Neumann *et al.*, 1997; Golz *et al.*, 2006). Interestingly, Type 1 interferons released from astrocytes in the spinal cord may interact with neuronal IFNRs in a manner that leads to decreased synaptic transmission in the dorsal horn resulting in hypoalgesia (Liu *et al.*, 2016).

The 2-photon imaging technology does not allow for information regarding the conduction velocity of the nerves being activated. In this study we conclude that C-fibers were stimulated because the majority of the IFN-activated fibers were subsequently activated by capsaicin, a selective C-fiber stimulant. In addition, most fibers that were activated were derived from small diameter neurons (see Table 2). It should be pointed out, however, that the IFNs did not exclusively activate C-fibers. The rt-PCR results reveal that many TRPV1-negative neurons express IFNRs. Moreover, we found examples of large diameter neurons activated by the type 1 IFNs, consistent with A-fiber activation (see video 1 and table 2). Most A-fibers in the lung are either slowly adapting or rapidly adapting low-threshold mechanosensors or “stretch receptors”. The properties of the presumed A-fibers that were activated by IFNs are unknown.

To our knowledge, the data presented here are the first to show that IFNs can cause the acute activation of sensory C-fiber nerve terminals directly within a tissue. We infused a bolus of IFN into a perfused and superfused trachea-lung preparation so the concentration of IFN at the given nerve terminal is unknown (some value less than the concentration infused into the trachea/lung). Nevertheless, the conclusion that the activation of the airway nerve terminals by IFNβ is secondary to stimulation of type 1 IFN receptors is supported by our findings with the IFNAR1 blocking antibody. The antibody blocked the response to IFNβ but not IFNγ or capsaicin supporting the selectivity in its blocking activity. Although the mechanism of IFNγ -induced activation of the nerves was not pursued here, it is consistent with expression of type 2 IFN receptors IFNGR1 and IFNGR2 shown in our published RNAseq analysis (Wang *et al.*, 2017). This is also consistent with our observation that IFNγ acutely stimulates a calcium rise in the nerve cell bodies isolated from mouse vagal ganglia (Wang *et al.*, 2017). IFNγ has also recently been shown to activate cell bodies of neurons dissociated from rat vagal nodose ganglia (Deng *et al.*, 2018).

The ionic mechanisms down-stream of type 1 IFNR activation that leads to action potential discharge in pulmonary sensory nerve terminals remains unknown. The observation that applying IFNβ directly to the isolated vagal ganglion acutely activated neurons indicates that the response evoked at the nerve endings in the lungs are unlikely dependent on stimulation of non-neural airway cells. Pharmacological data indicate that JAK activation is required for IFNβ-induced activation of vagal nerve terminals. Since we found that vagal C-fiber neurons selectively express JAK1 but not JAK2 or JAK3 (Wang *et al.*, 2017) we conclude that JAK1 most likely leads to as yet undefined signaling events that phosphorylate certain ion channel in the terminal membrane that cause membrane depolarization. In cortical pyramidal neurons, IFNβ leads to increases in neuronal excitability; an effect that may be secondary to PKC activation and the result of a concerted response of several disparate ion channels (Reetz *et al.*, 2014).

The electrophysiological approach (extracellular single fiber recording) to studying C-fiber activity provides detailed information regarding action potential firing frequencies, however it is time consuming with typically only one fiber studied per animal per day. This can become very costly when expensive cytokines are to be investigated. With GCaMP imaging, hundreds of airway specific fibers can be analyzed in a single experiment, making it very useful in determining the percentage of sensitive nerves in the lungs that were sensitive to the IFN. The efficacy of the IFNβ response, as indicated by fluorescence intensity, was similar to capsaicin. Although, the intensity of the fluorescence is roughly a function of the number of action potentials arising at the cell body (figure 2), due to the slow kinetics (we noted a decay constant of about 60 msec) it gives no indication of the frequency or pattern of action potential discharge. In a previous study, for example, we noted that similar intensities of fluorescence were evoked by intra-tracheal injection of sphinogosine-1 phosphate vs capsaicin (Patil *et al.*, 2019). When this was investigated electrophysiologically, however, capsaicin evoked a short duration high frequency (~20Hz) burst of action potential discharge compared to the lower frequency (5Hz) more persistent discharge of action potential evoked by shingosine-1 phosphate. To determine if the frequency of action potential discharge evoked by IFNβ was sufficient to cause nocifensive reflexes, we investigated its effect on breathing pattern. That IFNβ caused two classic vagal nocifensive responses, gaps in

breathing and augmented breaths (Chou *et al.*, 2008; Deng *et al.*, 2018; Han *et al.*, 2018) supports the conclusion that IFNβ -induced stimulation of nerve terminals is of an intensity that is physiologically relevant. When studying reflex behavior *in vivo* it is difficult to definitively ascribe the response to a specific afferent nerve subtype. Nevertheless, the gasping and apneas are most likely due to vagal afferent nerve activation and unlikely caused by activation of the very spare sensory innervation derived from DRG neurons. Since the effect can be mimicked with capsaicin, a selective C-fiber activator, it is likely that vagal C-fibers are involved, however, we cannot rule out a role for vagal A-fibers in the defensive reflex behaviors. The acute onset of the response, taken together with the results on receptor expression and vagal nerve activation, supports the hypothesis that IFNβ evoked the defensive reflexes by directly activating the vagal C-fiber terminals. That is not to say that on a longer time scale, interferons in the lungs won't also modulate respiratory reflexes indirectly via their effects on regulating immune and inflammatory responses.

While it is premature to extend these findings to the human condition, it is tempting to speculate that IFN-induced broncho-pulmonary C-fiber activation contributes to coughing that is commonly associated with respiratory viral infections. Other substances that are known to activate vagal C-fibers such as acids, bradykinin, ATP, capsaicin, and TRPA1 agonists all cause coughing when inhaled by human volunteers (Belvisi *et al.*; Canning *et al.*, 2014). A better understanding of the non-nuclear ionic events downstream from IFNR activation in C-fiber terminals that lead to action potential discharge may suggest new drug targets to block viral cough and thereby inhibit viral spreading. Vagal C-fiber activation can also lead to reflex bronchospasm, secretions, and dyspnea (Mazzone & Undem, 2016). While IFN-induced nocifensive sensations and reflexes may provide a modest beneficial effect in healthy individuals, the same sensations and reflexes may be exaggerated in children with airway hyperresponsiveness and asthma where viral infection may lead to exaggerated secretions and bronchoconstriction that can compromise lung function. Indeed, it has been estimated that about 80% of asthma attacks in children are associated with respiratory viral infections (Johnston *et al.*, 1995).

Supplementary Material

Refer to Web version on PubMed Central for supplementary material.

Acknowledgments

Funding

This work was funded by NIH, Bethesda Maryland (HLR01-137807). Dr. Patil was partially funded by the Johns Hopkins Division of Allergy and Clinical Immunology David Marsh Award. We thank Dr. Jeffrey Riggs and Brian Naiman (AstraZeneca) for their helpful guidance in using the IFNAR antibodies.

This work was funded by National Institutes of Health (R01HL137807) and M. Patil was partially funded by the David Marsh Fellowship Award.

Data Availability Statement

The data that support the findings of this study are available from the corresponding author upon reasonable request.

REFERENCES

Belvisi MG, Dubuis E & Birrell MA. Transient receptor potential A1 channels: insights into cough and airway inflammatory disease. Chest 140, 1040–1047.

Canning BJ, Chang AB, Bolser DC, Smith JA, Mazzone SB, McGarvey L & Panel CEC. (2014). Anatomy and neurophysiology of cough: CHEST Guideline and Expert Panel report. Chest 146, 1633–1648. [PubMed: 25188530]

Chen TW, Wardill TJ, Sun Y, Pulver SR, Renninger SL, Baohan A, Schreiter ER, Kerr RA, Orger MB, Jayaraman V, Looger LL, Svoboda K & Kim DS. (2013). Ultrasensitive fluorescent proteins for imaging neuronal activity. Nature 499, 295–300. [PubMed: 23868258]

Chou YL, Scarupa MD, Mori N & Canning BJ. (2008). Differential effects of airway afferent nerve subtypes on cough and respiration in anesthetized guinea pigs. Am J Physiol Regul Integr Comp Physiol 295, R1572–1584. [PubMed: 18768768]

Deng Z, Zhou W, Sun J, Li C, Zhong B & Lai K. (2018). IFN-gamma Enhances the Cough Reflex Sensitivity via Calcium Influx in Vagal Sensory Neurons. Am J Respir Crit Care Med 198, 868–879. [PubMed: 29672123]

Golz G, Uhlmann L, Ludecke D, Markgraf N, Nitsch R & Hendrix S. (2006). The cytokine/neurotrophin axis in peripheral axon outgrowth. Eur J Neurosci 24, 2721–2730. [PubMed: 17156198]

Grundy D. (2015). Principles and standards for reporting animal experiments in The Journal of Physiology and Experimental Physiology. J Physiol 593, 2547–2549. [PubMed: 26095019]

Han L, Limjunyawong N, Ru F, Li Z, Hall OJ, Steele H, Zhu Y, Wilson J, Mitzner W, Kollarik M, Undem BJ, Canning BJ & Dong X. (2018). Mrgprs on vagal sensory neurons contribute to bronchoconstriction and airway hyper-responsiveness. Nat Neurosci.

Johnston SL, Pattemore PK, Sanderson G, Smith S, Lampe F, Josephs L, Symington P, O'Toole S, Myint SH, Tyrrell DA & et al. (1995). Community study of role of viral infections in exacerbations of asthma in 9–11 year old children. BMJ 310, 1225–1229. [PubMed: 7767192]

Kim SH, Hadley SH, Maddison M, Patil M, Cha B, Kollarik M & Taylor-Clark TE. (2020). Mapping of Sensory Nerve Subsets within the Vagal Ganglia and the Brainstem Using Reporter Mice for Pirt, TRPV1, 5-HT3, and Tac1 Expression. eNeuro 7.

Kollarik M, Dinh QT, Fischer A & Undem BJ. (2003). Capsaicin-sensitive and -insensitive vagal bronchopulmonary C-fibres in the mouse. J Physiol 551, 869–879. [PubMed: 12909686]

Liu CC, Gao YJ, Luo H, Berta T, Xu ZZ, Ji RR & Tan PH. (2016). Interferon alpha inhibits spinal cord synaptic and nociceptive transmission via neuronal-glial interactions. Sci Rep 6, 34356. [PubMed: 27670299]

Mazzone SB, Tian L, Moe AAK, Trewella MW, Ritchie ME & McGovern AE. (2020). Transcriptional Profiling of Individual Airway Projecting Vagal Sensory Neurons. Mol Neurobiol 57, 949–963. [PubMed: 31630330]

Mazzone SB & Undem BJ. (2016). Vagal Afferent Innervation of the Airways in Health and Disease. Physiol Rev 96, 975–1024. [PubMed: 27279650]

Nassenstein CT-CT, Myers AC, Ru F, Nandigama R, Bettner W, Undem BJ. (2010). Phenotypic distinctions between neural crest and placodal derived vagal C-fibers in mouse lungs. J Physiol 588, 4769–4783. [PubMed: 20937710]

Neumann H, Schmidt H, Wilharm E, Behrens L & Wekerle H. (1997). Interferon gamma gene expression in sensory neurons: evidence for autocrine gene regulation. J Exp Med 186, 2023–2031. [PubMed: 9396771]

Patil MJ, Meeker S, Bautista D, Dong X & Undem BJ. (2019). Sphingosine-1-phosphate activates mouse vagal airway afferent C-fibres via S1PR3 receptors. J Physiol 597, 2007–2019. [PubMed: 30793318]

Peng L, Oganesyan V, Wu H, Dall'Acqua WF & Damschroder MM. (2015). Molecular basis for antagonistic activity of anifrolumab, an anti-interferon-alpha receptor 1 antibody. MAbs 7, 428–439. [PubMed: 25606664]

Reetz O, Stadler K & Strauss U. (2014). Protein kinase C activation mediates interferon-beta-induced neuronal excitability changes in neocortical pyramidal neurons. J Neuroinflammation 11, 185. [PubMed: 25359459]

Schneider WM, Chevillotte MD & Rice CM. (2014). Interferon-stimulated genes: a complex web of host defenses. Annu Rev Immunol 32, 513–545. [PubMed: 24555472]

Secombes CJ & Zou J. (2017). Evolution of Interferons and Interferon Receptors. Front Immunol 8, 209. [PubMed: 28303139]

Van Rompaey L, Galien R, van der Aar EM, Clement-Lacroix P, Nelles L, Smets B, Lepescheux L, Christophe T, Conrath K, Vandeghinste N, Vayssiere B, De Vos S, Fletcher S, Brys R, van 't Klooster G, Feyen JH & Menet C. (2013). Preclinical characterization of GLPG0634, a selective inhibitor of JAK1, for the treatment of inflammatory diseases. J Immunol 191, 3568–3577. [PubMed: 24006460]

Vikman K, Robertson B, Grant G, Liljeborg A & Kristensson K. (1998). Interferon-gamma receptors are expressed at synapses in the rat superficial dorsal horn and lateral spinal nucleus. J Neurocytol 27, 749–759. [PubMed: 10640190]

Wang J, Kollarik M, Ru F, Sun H, McNeil B, Dong X, Stephens G, Korolevich S, Brohawn P, Kolbeck R & Undem B. (2017). Distinct and common expression of receptors for inflammatory mediators in vagal nodose versus jugular capsaicin-sensitive/TRPV1-positive neurons detected by low input RNA sequencing. PLoS One 12, e0185985.

Key points

- Type I interferon receptors are expressed by the majority of vagal C-fiber neurons innervating the respiratory tract
- Interferon alpha and beta acutely and directly activate vagal C-fibers in the airways.
- The interferon-induced activation of C-fibers occurs secondary to stimulation of type 1 interferon receptors
- Type 1 interferons may contribute to the symptoms as well as the spread of respiratory viral infections by causing coughing and other defensive reflexes associated with vagal C-fiber activation

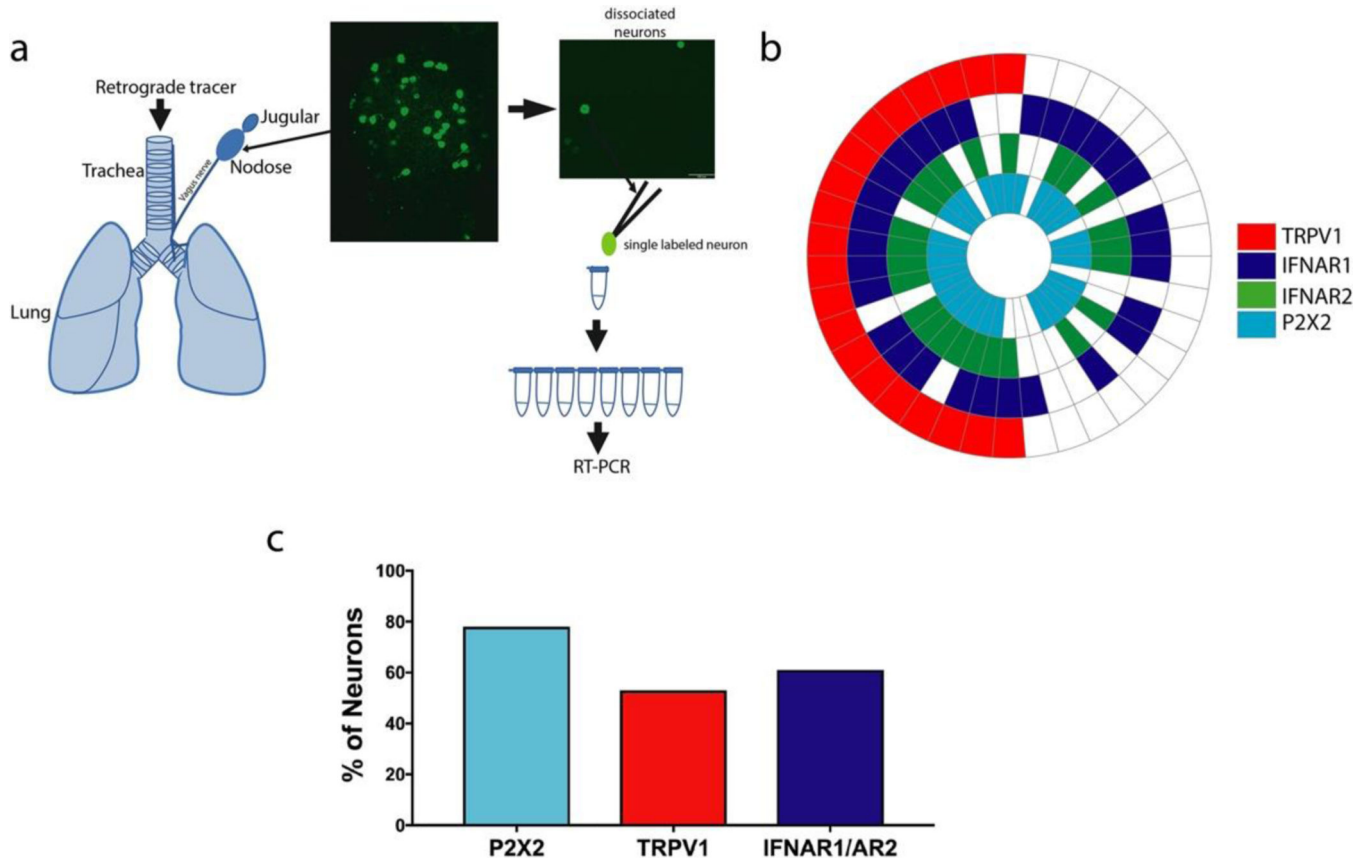

FIG 1. Airway-specific neurons express interferon Type I receptor mRNA.

a. Schematic of labeling of the mouse airways with WGA 488 tracer injected in the airways. WGA 488 labeled lung-specific neurons are green in the nodose ganglia picture and the dissociated neurons on a coverslip are picked one at a time using a glass pipette to perform RT-PCR. White line in the ganglia image represents 100 μm. **b**. Expression wheel of mRNA expression in 38 airway-specific neurons (38 neurons from 4 mice). Each section represents one cell. **c**. Percentage of neurons expressing, P2X2 (marker for nodose neurons) TRPV1 (marker for a subset of C-fiber neurons), and IFN receptor genes (aggregate data of 38 neurons from 4 mice).

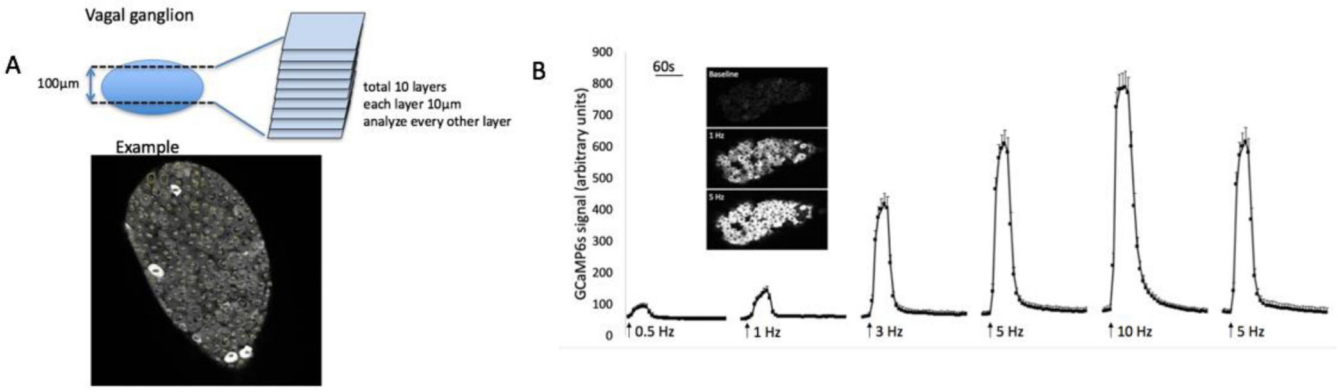

FIG 2. 2-Photon imaging of nodose ganglia during electrical stimulation of the vagus nerve leads to an increase in GCaMP6s signal.

A. Illustration of how the neurons are analyzed. In the example shown, there are 218 neurons, 4 of which are positive (fluorescing). In general, 800–1200 neurons are evaluated in each ganglion (5 sections). White bar on the ganglia image represents 100 µm. **B**. Graph showing GCaMP6s mean intensity signal during electrical stimulation of the vagus nerve, from a Pirt-cre/GCaMP6s mouse, in an *ex vivo* preparation. GCaMP6s signal peaks after 20s, and takes time to decay, consistent with GCaMP6s properties. Each stimulation was for 20s. N=161 nodose neurons from 3 ganglia of 3 mice. The decay of the fluorescence after the 10 Hz stimulation ended had a constant of 60±2.8 ms-1 (mean and SD, n=161 neurons from 3 mice). The decay constant for each neuron was calculated by linear regression as a slope of the initial linear portion of log transformed decay curve.

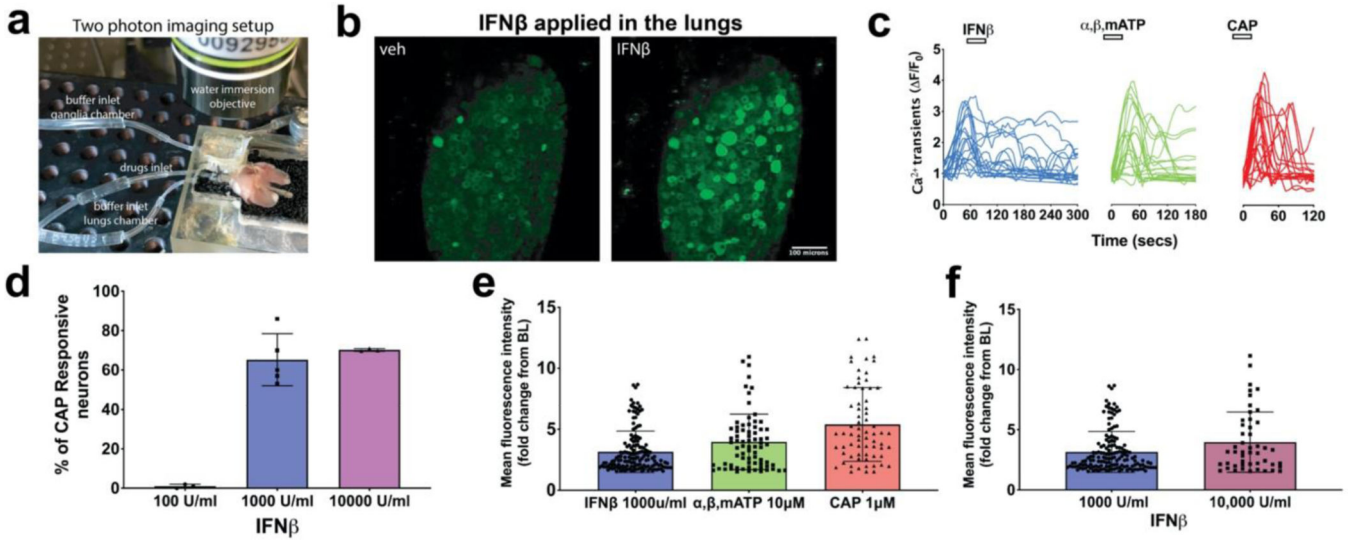

FIG 3: IFNβ, Type I interferon activates airway nodose C-fibers, visualized by two-photon.

a. Photograph showing the two-photon imaging setup with the *ex vivo* preparation of lungs, vagus nerve, and vagal ganglia in the chamber. **b**. Z stacked images of the same nodose ganglia after application of vehicle and then application of IFNβ (1000 U/ml). 1 ml of vehicle or IFNβ was delivered into the lungs in 1 min and the response of neurons from the nodose ganglia recorded for a total of 6mins (Video 1 in supplementary material). **c**. Graphs showing calcium transients caused by action potentials arising from lung terminals of 20 representative neurons that were responsive to IFNβ, α,β,mATP (10uM) and CAP (1uM). X axis denotes the time and Y axis denotes the fluorescence intensity values calculated as change from baseline ($\Delta F/F_0$), (n=~400 neurons from n=4 mice). **d**. Graph of IFNβ sensitive neurons, plotted as percentage of capsaicin (CAP) responsive neurons from 4 independent experiments (with 4 different mice preparations) with different concentrations of IFNβ (pooled data from 4 mice showing mean and SD). **e**. Graph showing the mean intensity values of all the responsive neurons to the X axis mentioned agonists (pooled data from n=~400 neurons from 4 mice, showing mean and SD). **f**. Mean fluorescent intensities of nodose ganglia responsive neurons to 1000 and 10,000 U/ml concentrations of IFNβ (aggregate data from independent observations for each concentration, n=3 mice for each concentration of IFNβ, showing mean and SD). A t-test was used to compare paired observations and One-way ANOVA test was used to compare unpaired groups using GraphPad prism software (Bonferroni correction).

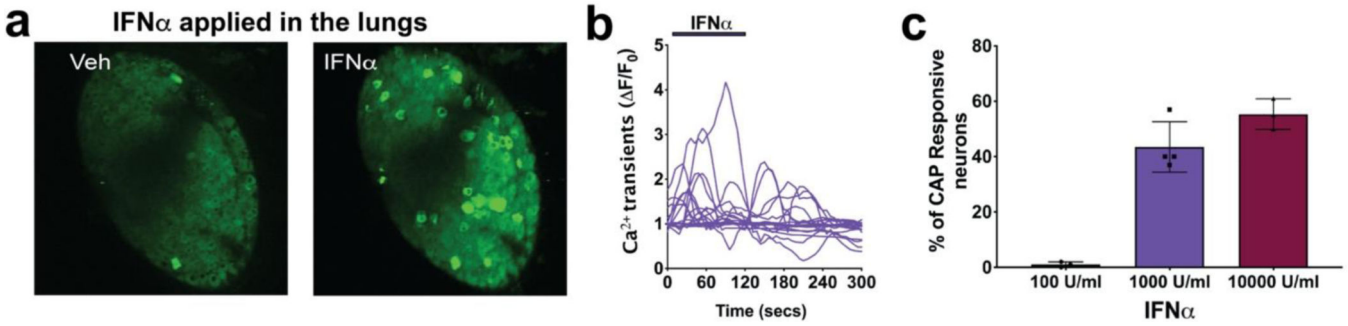

FIG 4. Application of IFNα in the lungs activates airway nodose C-fibers, visualized by two-photon.

a. Z stacked images of the same nodose ganglia after application of vehicle and then application of IFNα (1000 U/ml). 1 ml of vehicle or IFNα was delivered into the lungs in 1 min and the response of neurons from the nodose ganglia recorded for a total of 6mins. White bar on the ganglia images represents 100 μm **b**. Graphs showing calcium transients caused by action potentials arising from lung terminals of 20 representative neurons that were responsive to IFNα (1000 U/ml). X axis denotes the time and Y axis denotes the fluorescence intensity values calculated as change from baseline ($\Delta F/F_0$), n=~300 neurons from 3 mice. **c**. Graph showing the percentage of capsaicin (CAP) responsive neurons from 3 independent experiments with different concentrations of IFNα (n=~300 neurons from 3 mice, showing mean and SD). A t-test using GraphPad prism software (Bonferroni correction) was used throughout to compare unpaired groups.

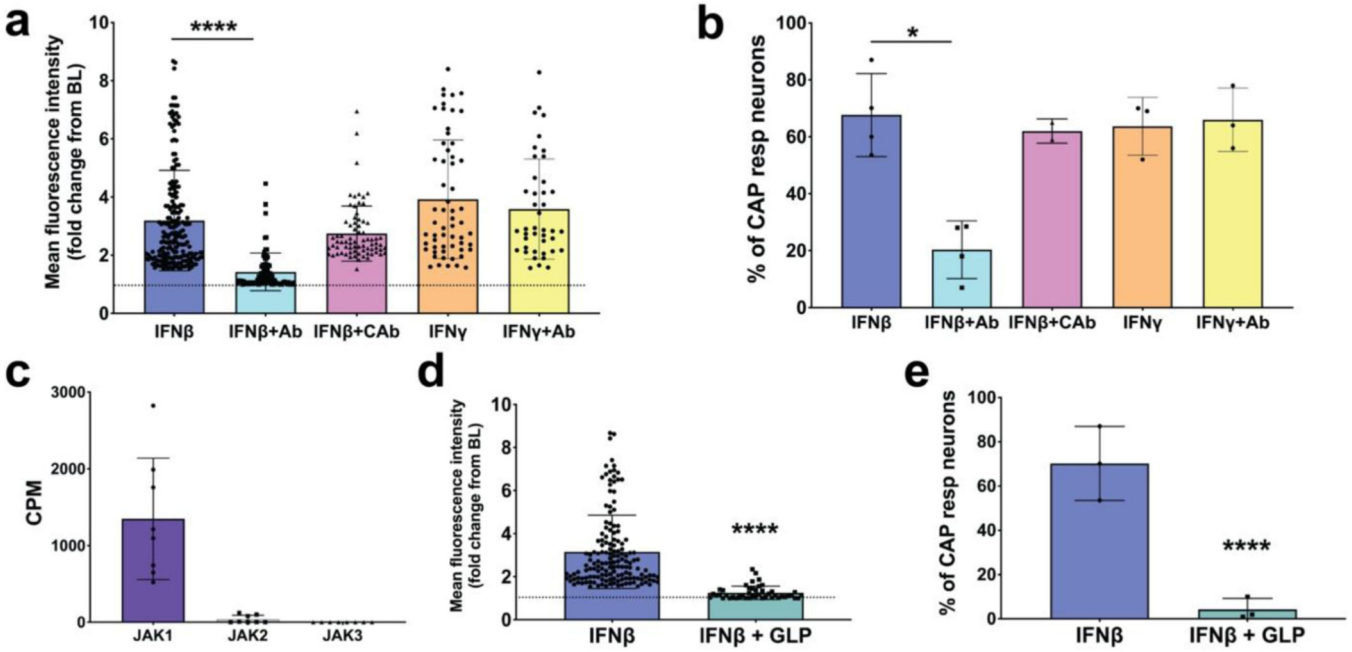

FIG 5: Type I Interferons activate airway nodose ganglia afferents via IFN Type I receptors signaling through JAK1 kinase.

a. Response of airway sensory nerves to IFNβ (1000 U/ml applied to the lungs via the trachea) in the absence and presence of IFN type 1 receptor blocking antibody (anti-IFNAR1, 1ug/ml applied 15 minutes before IFN treatment) or isotype control antibody; the response to IFN**γ** (dose) in the absence and presence of the IFN1 blocking antibody is also shown. **b**. Graph showing the % of capsaicin (CAP) responsive neurons from experiments performed in panel a. **c**. Bar graph showing the presence of JAK1, JAK2 and JAK3 transcripts, measured as CPM, from nodose ganglia found using RNAseq. **d**. Graph comparing the mean fluorescence intensities after neuronal activation by IFNβ (1000 units/ml) in the absence and presence of the JAK1 inhibitor filgotinib/GLPG0634 (1μM) (dose perfused for 15 min before IFNβ) pretreatment to the airway afferents and then the application of IFN β. **e**. Graph showing % of CAP responsive neurons from experiments performed in panel d. (n=~400 neurons from n=4 mice for each treatment). All graphs show mean and SD. The asterisk denotes significant difference (* P< 0.05 and **** P< 0.0001) determined with unpaired One-way ANOVA test using GraphPad prism software (Bonferroni correction) was used throughout to compare unpaired groups.

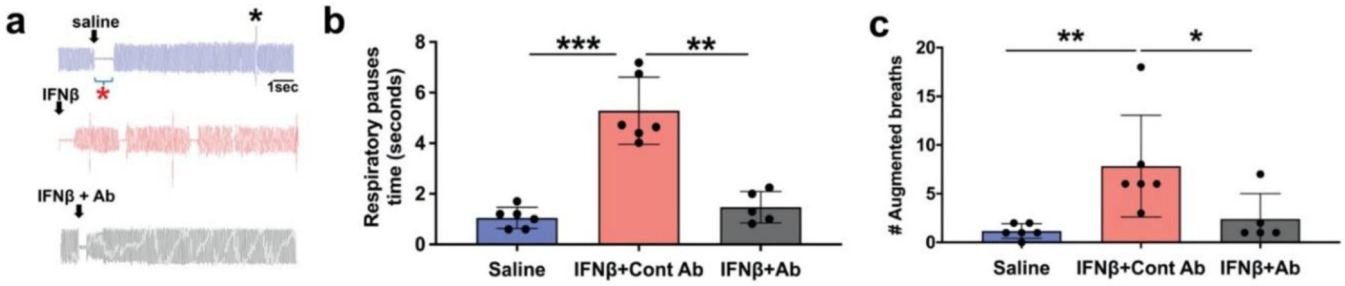

FIG 6. Delivery of IFNb into the mouse airways causes defensive reflexes that require interferon type I receptors.

a. Representative traces of pulmonary airflow waveforms from mice intratracheally treated with 2ul of saline(blue), IFNβ (2000U, red), and IFNβ + IFN type I receptor blocking antibody (black). The blocking antibody (1mg/kg) was given to the mice i.p. 4 hours before the experiment. Red asterisk denotes a respiratory pause and black shows an augmented breath **b**. Summary of the total duration of respiratory pauses during a 15-minute interval immediately after administration of 2ul of saline(blue), IFNβ (2000U), and IFNβ + IFN type I receptor blocking antibody. (graph shows mean and SD, n=6 in saline and IFNβ groups and n=5 in IFNb + IFN type I receptor blocking antibody group). IFNβ significantly increased the duration of respiratory pauses when delivered intratracheally in mice (***P<0.0002). IFN type I receptor blocking antibody was able to significantly block the IFNβ effect (**P<0.005). **c**. Summary of the total number of respiratory pauses during a 15-minute interval immediately after administration of 2ul of saline(blue), IFNβ (2000U), and IFNβ + IFN type I receptor blocking antibody. (graph shows mean and SD, n=6 in saline and IFNβ groups and n=5 in IFNβ + IFN type I receptor blocking antibody group). IFNβ significantly increased the duration of augmented breaths when delivered intratracheally in mice (**P<0.005). IFN type I receptor blocking antibody was able to significantly block the IFNβ effect (*P<0.01). A one-way ANOVA test using GraphPad prism software was used throughout to compare unpaired groups.

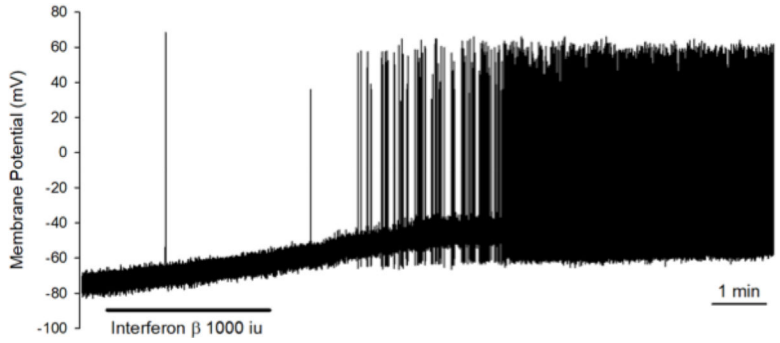

FIG 7: Direct application of IFNβ on the nodose ganglia and dissociated nodose ganglia neurons causes activation and action potential discharge.

IFNβ (1000U/ml) induced membrane depolarization (from −63.9±5 to −52.9±3.2 mV, n=7, P=0.009 by paired t-test) and action potential discharge in 4 out of 7 neurons with the mean peak frequency at 3.9±3.2 Hz. The tracing shown here is the membrane potential recording obtained from a capsaicin-sensitive nodose neuron using the perforated whole-cell patch clamp technique. The duration of IFNβ application by bath perfusion is indicated by the horizontal bar. The peak frequency of AP firing in this neuron is 9Hz.

TABLE 1.

Single cell RT-PCR primer sequences

Gene	Primer	Sequence	Product length
β Actin	Forward (5'–3') Reverse (3'–5')	CTG GTC GTC GAC AAC GGC TCC GCC AGA TCT TCT CCA TG	302 bp
IFNAR1	Forward (5'–3') Reverse (3'–5')	TCG AAC AAA AGA CGA GGC GA GGG CTC ATG TGA GCT GTG TA	198 bp
IFNAR2	Forward (5'–3') Reverse (3'–5')	AGG GGA CAG CGT TAG GAA GA AAA CCT AGC CAT ACC TGA TTC CT	193 bp
P2X2	Forward (5'–3') Reverse (3'–5')	GGG GCA GTG TAG TCA GCA TC TCA GAA GTC CCA TCC TCC A	241 bp
TRPV1	Forward (5'–3') Reverse (3'–5')	TCA CCG TCA GCT CTG TTG TC GGG TCT TTG AAC TCG CTG TC	285 bp

TABLE 2.

Percentages of the size of IFNβ responsive neurons from the vagal ganglia

Neuronal diameter	Small (10–15μm)	Medium (15–25μm)	Large (>25μm)
% IFNβ +	80%	18%	2%

Neuronal diameters of all type I IFN responsive neurons (n=300)